心筋肥大から心不全への遷展に伴う膜電流の経時的変化 — モノクロタリン誘起肺高血圧ラットにおける研究

李 鍾國、児玉 逸雄、本荘 晴朗、安野 尚史、神谷 香一郎、外山 淳治。

主論文

# Stage-dependent changes in membrane currents in rats with monocrotaline-induced right ventricular hypertrophy

JONG-KOOK LEE,[1] ITSUO KODAMA,[2] HARUO HONJO,[2] TAKAFUMI ANNO,[3] KAICHIRO KAMIYA,[1] AND JUNJI TOYAMA[1]

*Departments of [1]Circulation and [2]Humoral Regulation, Research Institute of Environmental Medicine, Nagoya University, Nagoya 464-01; and [3]Aichi Prefectural Center for Health, Nagoya 460, Japan*

**Lee, Jong-Kook, Itsuo Kodama, Haruo Honjo, Takafumi Anno, Kaichiro Kamiya, and Junji Toyama.** Stage-dependent changes in membrane currents in rats with monocrotaline-induced right ventricular hypertrophy. *Am. J. Physiol.* 272 (*Heart Circ. Physiol.* 41): H2833–H2842, 1997.— Sequential changes in action potential configuration, 4-aminopyridine-sensitive transient outward current ($I_{to}$), and L-type calcium current ($I_{Ca}$) in association with hypertrophy were investigated in ventricular myocytes from rats with monocrotaline (MCT)-induced pulmonary hypertension. The tissue weight ratio of right ventricle (RV) to left ventricle plus septum 14 and 28 days after a subcutaneous injection of MCT increased by 29.7 and 77.2%, respectively. Action potential duration (APD) of RV cells from MCT rats increased progressively, prolonged by 73.2 and 92.2% on *days 14* and *28*, respectively. The current density of $I_{to}$ in RV cells from MCT rats on *day 14* (32.5 ± 4.5 pA/pF, $n = 13$) was significantly larger than in controls (26.8 ± 4.5 pA/pF, $n = 8$; $P < 0.05$). On *day 28*, however, $I_{to}$ density in MCT rats (15.3 ± 4.6 pA/pF, $n = 9$) was significantly less than in controls (27.3 ± 4.2 pA/pF, $n = 10$; $P < 0.05$). There were no differences in the voltage dependence of steady-state activation and inactivation of $I_{to}$ between MCT and control rats. $I_{Ca}$ density in MCT rats on *day 14* (15.7 ± 2.6 pA/pF, $n = 10$) was significantly larger than in controls (10.0 ± 2.3 pA/pF, $n = 10$; $P < 0.05$), but there was no significant difference in $I_{to}$ density between MCT rats (8.3 ± 3.7 pA/pF, $n = 10$) and controls (11.6 ± 3.0 pA/pF, $n = 10$) on *day 28*. These findings suggest that hypertrophy of mammalian hearts may cause stage-dependent changes in $I_{to}$ and $I_{Ca}$ density of ventricular myocytes. The APD prolongation in the early stage of hypertrophy may be caused mainly by an increase in $I_{Ca}$ density, whereas the APD prolongation in the late stage may be ascribed to a reduction in $I_{to}$ density.

action potential; transient outward current; calcium current

CARDIAC HYPERTROPHY is an adaptive response of the heart to pressure and volume overloads. The most consistent electrical abnormality in association with hypertrophy of ventricular myocytes is prolongation of action potential duration (APD) (2, 12). As to the exact ionic mechanisms responsible for the APD prolongation, however, much remains to be clarified. Many investigators have examined the 4-aminopyridine (4-AP)-sensitive and intracellular calcium-independent component of transient outward current ($I_{to}$) and L-type calcium current ($I_{Ca}$) in hypertrophied cardiac cells, because the currents play an important role in repolarization of action potential in most animal species, including rats (3, 5, 6, 13, 15, 26, 28, 29), guinea pigs (17, 25), cats (7, 14, 27), dogs (16), and humans (4, 20).

It was shown in experiments on rat hearts with hypertrophy secondary to pressure (28) or volume overload or to hormonal intervention (29) or with genetically determined hypertension (6) that the current density of $I_{to}$ is reduced compared with controls. Opposite findings indicating an increase of $I_{to}$ density, however, have been presented by other investigators in hypertrophied ventricular myocytes from cats (27) and rats (15). Data on $I_{Ca}$ in experimentally induced hypertrophy are also diverse; $I_{Ca}$ density was shown to be increased (13, 25), decreased (17), or unchanged (5, 7, 14) in rats, cats, or guinea pigs. Different pathological processes in different hypertrophy models might result in these discrepancies. In these previous reports, data were obtained only at a certain stage of hypertrophy in each model. At the present time, however, little information is available about the chronological changes of membrane currents with the development of hypertrophy. We hypothesized that such a variation of hypertrophy-induced changes in $I_{to}$ and $I_{Ca}$ density may reflect stage-dependent changes in the currents.

In rats, a parenteral dose of monocrotaline (MCT), a pyrrolizidine alkaloid found in the leaves and seeds of the plant *Crotalaria spectabilis*, is known to cause pulmonary vascular damage and pulmonary hypertension within a few weeks (10, 18, 19). The damage includes swelling of capillary endothelial cells, lesions of the arterial media, and accumulation of platelet thrombi in blood vessels. The hemodynamic loading, in turn, results in a marked right ventricular hypertrophy, leading to right-sided congestive heart failure in several weeks. Because progressive right ventricular hypertrophy can be produced in such a short period with minimal pathological changes in the left ventricle, this noninvasive and nongenetic model is suitable for chronological investigation of action potentials and ionic currents over the entire time course of hypertrophy.

In the present study, we examined the sequential changes in action potential configuration, $I_{to}$, and $I_{Ca}$ in rat myocytes with the use of the whole cell patch-clamp technique at various stages of MCT-induced right ventricular hypertrophy. The results revealed that myocardial hypertrophy secondary to pressure overload causes complex stage-dependent changes in ionic currents of ventricular cells.

## MATERIALS AND METHODS

*Animals.* Five-week-old male Wistar rats weighing 170–190 g were treated with MCT (Sigma, St. Louis, MO) to produce pulmonary hypertension as described previously (10,

18, 19). A single dose of 60 mg/kg MCT was injected subcutaneously into the interscapular region. MCT was dissolved in 1 N HCl neutralized with 0.5 N NaOH and diluted with sterile distilled water to obtain a 2% solution. In control rats of corresponding age and weight, saline was injected instead of MCT. The rats were allowed to eat freely from a supply of standard rat chow and were weighed daily during the subsequent 4 wk. The animals were killed under ether anesthesia on the day of MCT or saline injection (*day 0*) or 7, 14, 21, or 28 days after the injection. The hearts were removed quickly and were used for estimation of right ventricular (RV) hypertrophy and for cell isolation. RV hypertrophy was estimated by determining the tissue weight ratio of the RV free wall to the left ventricular free wall plus septum (LV + S).

*Cell isolation.* Single myocytes were isolated enzymatically from the RV and the LV. In brief, the excised hearts were perfused on Langendorff apparatus with the following solutions in sequence: *1*) normal Tyrode solution gassed with 100% $O_2$ at 37°C for 2 min to wash the blood from the heart, *2*) nominally $Ca^{2+}$-free Tyrode solution for 5 min, *3*) enzyme solution containing collagenase (80–100 IU/ml; Yakult) for 4–5 min, and *4*) modified Kraftbrühe (KB) solution for 3 min. The RV and LV free walls were then harvested separately from the heart and were minced in the modified KB solution to disperse single myocytes. The cells were kept in the storage solution at 4°C and were studied within 6 h after isolation.

*Solutions.* The composition of the normal Tyrode solution was (in mM) 143 NaCl, 5.4 KCl, 1.8 $CaCl_2$, 0.25 $MgCl_2$, 0.25 $NaH_2PO_4$, 5 *N*-2-hydroxyethylpiperazine-*N*′-2-ethanesulfonic acid (HEPES), and 5 glucose (pH 7.4 with NaOH). The nominally $Ca^{2+}$-free Tyrode solution was prepared by omitting $CaCl_2$ from the normal Tyrode solution. The composition of KB solution was (in mM) 70 KOH, 40 KCl, 50 L-glutamic acid, 20 taurine, 10 $KH_2PO_4$, 0.5 $MgCl_2$, 11 glucose, 0.5 ethylene glycol-bis(β-aminoethyl ether)-*N*,*N*,*N*′,*N*′-tetraacetic acid (EGTA), and 10 HEPES (pH 7.4 with KOH). For the recording of action potentials, cells were perfused with the normal Tyrode solution. The pipette solution was composed of (in mM) 80 KCl, 60 KOH, 40 aspartate, 5 HEPES, 10 EGTA, 5 MgATP, 5 sodium creatine phosphate, and 0.65 $CaCl_2$ (pH 7.3 with KOH). For the measurements of whole cell $I_{to}$ ($Ca^{2+}$-insensitive component of $I_{to}$), 0.3 mM $CdCl_2$ and 10 μM tetrodotoxin (TTX) were added to the external solution to block calcium current and fast sodium current. For the recording of $I_{Ca}$, potassium in the external and pipette solutions was replaced by cesium, and 10 μM TTX was added to the external solution to avoid contamination by potassium and sodium currents.

*Electrophysiological measurements.* Membrane potential and currents of single ventricular cells were recorded with the use of the gigaohm seal, patch-clamp technique in the whole cell configuration with an Axopatch-1D amplifier (Axon Instruments, Burlingame, CA) (8). The temperature of the bath solution was maintained at 35°C throughout the experiments. The resistance of patch pipettes ranged from 2 to 3 MΩ when filled with the normal internal solution. The cell membrane capacitance ($C_m$) was determined by applying a 10-mV hyperpolarizing voltage-clamp step from a holding potential ($V_h$) at −50 mV and integrating the area under the capacity transient. The series resistance was compensated by minimizing the duration of the capacitive surge on the current tracings. The junctional potential between the pipette and the bath solution was −4 mV, and it was not corrected.

$I_{to}$ was measured in the voltage-clamp mode by applying 300-ms depolarizing pulses to a test potential ranging from −50 to +50 mV in 10-mV steps from a $V_h$ of −80 mV at an interval of 10 s (0.1 Hz). The depolarization to a level more positive than −30 mV elicited an outward current of rapid activation followed by slower inactivation. This time-dependent current was eliminated nearly completely after application of 2 mM 4-AP, indicating that this outward current is a 4-AP-sensitive $I_{to}$. The amplitude of $I_{to}$ was measured as the difference between the peak of the outward current and the minimum current level during the depolarizing pulse after the peak. The voltage dependence of $I_{to}$ activation was estimated by calculating the chord conductance ($G$) from $I_{to}$ amplitude at various voltages, assuming a reversal potential ($V_{rev}$) of −75 mV (1). The maximum chord conductance ($G_{max}$) was determined with Boltzmann fit according to the following equation

$$G = G_{max}/[1 + \exp[(V_{0.5} - V)/k]]$$

where $V_{0.5}$ is the potential at which the conductance is half-maximally activated and $k$ is the slope factor describing the steepness of the activation curve. In experiments to examine the voltage dependence of steady-state inactivation, a test depolarization to +30 mV was preceded by a 1-s conditioning pulse to various voltage levels ranging from −100 to 0 mV in 10-mV steps.

$I_{Ca}$ was recorded by applying 300-ms depolarizing pulses to a test potential ranging from −60 to +60 mV in 10-mV steps from a $V_h$ of −80 mV at an interval of 10 s (0.1 Hz). The amplitude of $I_{Ca}$ was measured as the difference between the peak inward current and the steady-state current during the depolarizing voltage-clamp pulses. The current amplitude of $I_{Ca}$ decreases during the course of whole cell clamp experiments. We found that this decline of $I_{Ca}$ averaged 18% over 15 min. All the recordings of $I_{Ca}$ were, therefore, performed exactly at 3–5 min after the establishment of a gigaohm seal.

The current signal was filtered by a Bessel-type, low pass filter with a cutoff frequency of 10 kHz (−3 dB). During an experiment, membrane potential and current were monitored on a storage oscilloscope (Tektronix 5000 series). Data were sampled directly into a computer with pClamp or Axotape software (Axon Instruments).

*Statistics.* Data are expressed as means ± SE unless otherwise specified. The numbers of observations for action potentials and ionic currents were all single measurements in single cells. Statistical analysis was performed with the use of one-way analysis of variance with multiple comparisons. Differences were considered significant at $P < 0.05$.

## RESULTS

*Characteristics of experimental animals.* Figure 1*A* shows the weight ratio of RV to LV + S. The ratio in control rats ($n$ = 8–13) was maintained at an almost constant level throughout the entire observation period. In contrast, the ratio in MCT-treated rats ($n$ = 8–13) increased progressively from the second to the fourth week after injection.

Figure 1*B* illustrates sequential changes in body weight. In 10 control rats, the value increased gradually for 4 wk after injection, reflecting normal growth of the animals. In 12 MCT-treated rats, an increase in body weight similar to that in controls was observed during the initial 3 wk after injection. From the fourth week, however, the body weight of MCT-treated rats decreased. In the fifth week, 11 out of the 12 MCT-treated rats showed physical signs of right-side heart failure, including tachypnea, ascites, pleural effusion,

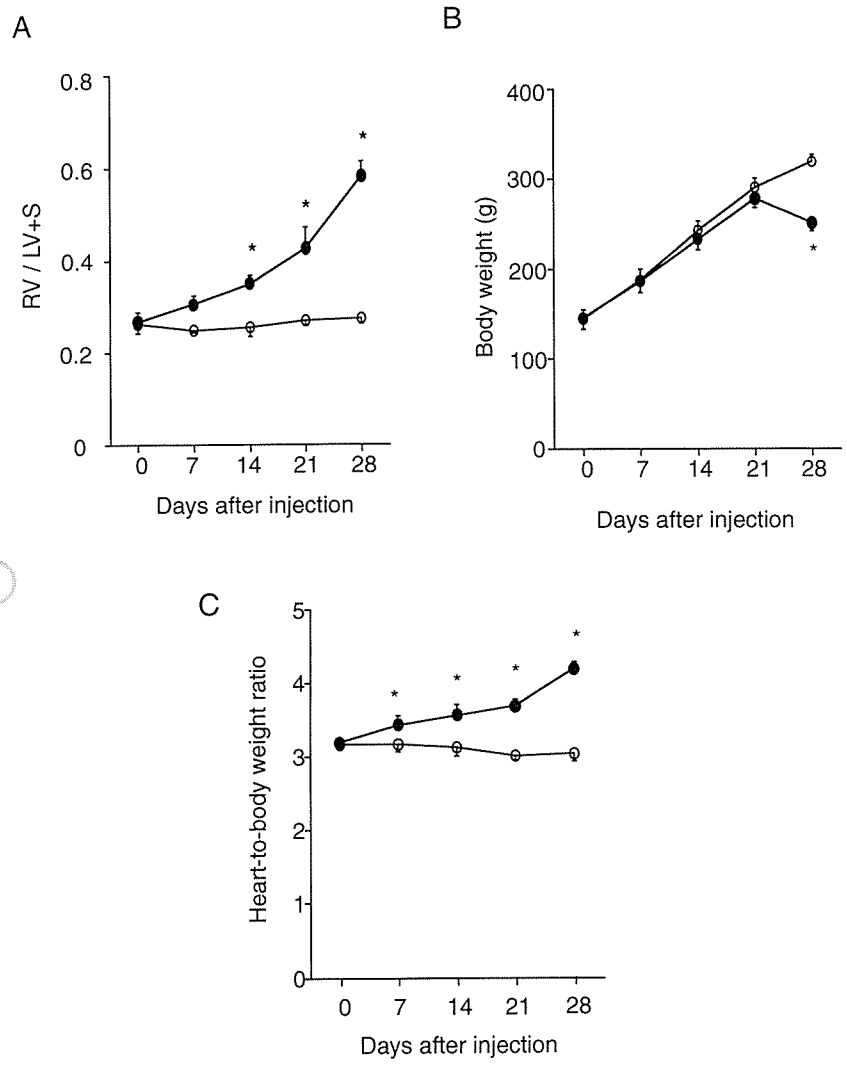


Fig. 1. Characteristics of experimental animals. *A*: tissue weight ratio of right ventricle (RV) to left ventricle plus interventricular septum (LV + S); *B*: body weight; *C*: heart-to-body weight ratio. Values are means ± SE ($n$ = 8–13) from control (○) and monocrotaline (MCT)-treated (●) rats. *Significantly different from control at $P < 0.05$.

edematous extremities, and piloerection. These facts indicate that the MCT-treated rats were in compensated condition during the initial 3 wk after injection but were decompensated from the fourth week.

Figure 1*C* shows heart-to-body weight ratios. In control rats, the ratio was constant during the 4 wk of observation. In MCT-treated rats, the ratio increased progressively. The average increase in the ratio compared with controls on *days 14* and *28* after injection was 14.4 and 38.1%, respectively.

*$C_m$ and action potential.* $C_m$, which reflects cell size, was measured in single RV or LV cells isolated from control and MCT-treated rats on *days 0*, *7*, *14*, *21*, and *28* after injection. In control rats, $C_m$ in both RV and LV cells was constant within a range from 89.6 to 93.3 pF throughout the observation period (Table 1). In MCT-treated rats, $C_m$ of RV cells increased progressively from the second week and reached 145.7 pF on *day 28*, whereas $C_m$ of LV cells was virtually unaffected (Table 1).

Transmembrane action potentials of these cells were recorded under constant stimulation at 1.0 Hz. Representative recordings are shown in Fig. 2. Action potentials of the RV cells from MCT-treated rats on *days 14* and *28* after injection were appreciably longer than those from control rats on the corresponding days. In contrast, the action potential of an LV cell from a MCT-treated rat on *day 28* had similar duration to that from a control rat. Table 2 summarizes action potential parameters of RV and LV cells from control and MCT-treated rats on *day 28* after injection. In RV cells, APD at 25, 50, and 90% repolarization ($APD_{25}$, $APD_{50}$, and $APD_{90}$, respectively) of MCT-treated groups were all significantly longer than those of controls. In LV cells, there was no significant difference in these APD parameters between control and MCT-treated groups. The

Table 1. *Cell capacitance of right and left ventricular myocytes*

| | RV | | | LV | | |
|---|---|---|---|---|---|---|
| Day | $n$ | Control | Monocrotaline | $n$ | Control | Monocrotaline |
| *0* | 8 | 89.6 ± 5.9 | 98.5 ± 4.0 | 7 | 97.2 ± 6.8 | 97.9 ± 8.2 |
| *7* | 8 | 90.7 ± 7.2 | 100.1 ± 5.2 | 7 | 98.3 ± 5.0 | 99.6 ± 6.3 |
| *14* | 9 | 92.2 ± 9.5 | 128.3 ± 15.8* | 9 | 99.8 ± 12.3 | 101.3 ± 15.8 |
| *21* | 16 | 93.2 ± 11.7 | 138.5 ± 16.7* | 9 | 102.3 ± 8.9 | 102.6 ± 12.3 |
| *28* | 10 | 93.3 ± 15.8 | 145.7 ± 21.2* | 11 | 99.1 ± 10.2 | 100.1 ± 6.5 |

Values are means ± SE; $n$, no. of cells. RV, right ventricle; LV, left ventricle. *Significantly different from control at $P < 0.05$.

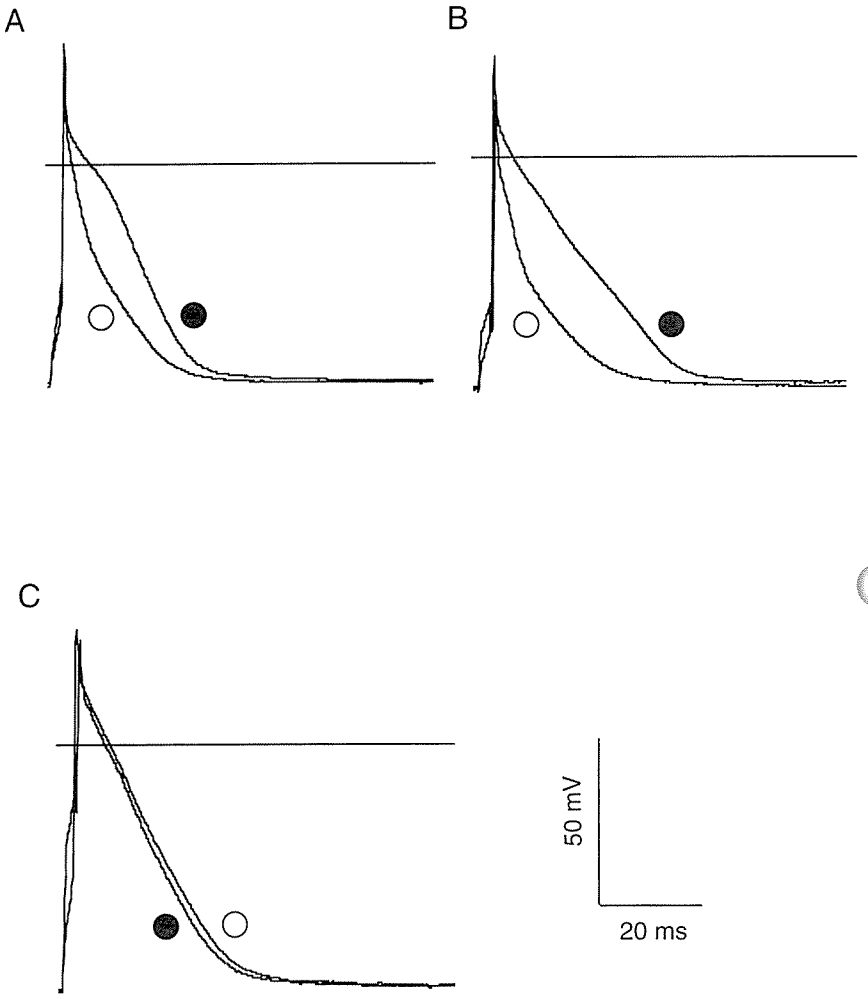


Fig. 2. Action potentials of ventricular myocytes. Recordings obtained in representative single ventricular cells isolated from control (○) and MCT-treated rats (●) are superimposed. *A*: RV cells at *day 14* after injection. *B*: RV cells at *day 28* after injection. *C*: LV cells at *day 28* after injection. Cells were stimulated at 1.0 Hz.

resting membrane potential (RMP) and the amplitude of action potential (AMP) were unaffected by MCT treatment in either RV or LV cells.

Figure 3 illustrates sequential changes in $APD_{90}$ in all control and MCT-treated rats tested ($n$ = 8–16 for each group on the respective day). In control rats, the $APD_{90}$ of RV cells on *day 0* was significantly shorter than that of LV cells and did not change throughout the observation period. In MCT-treated rats, the $APD_{90}$ of RV cells was prolonged significantly on *day 14*, and the prolongation was progressively enhanced during the subsequent period. On *day 28*, the $APD_{90}$ of RV cells increased to 192% of control. The $APD_{90}$ of LV cells from MCT-treated rats remained constant throughout the observation period, similar to control rats.

*$I_{to}$ in normal and hypertrophied myocytes.* Figure 4*A* shows representative current tracings of $I_{to}$ in RV myocytes from control and MCT-treated rats on *day 14* after injection. $C_m$ was 82.6 pF in the control cell and 85.2 pF in the MCT-treated cell. $I_{to}$ was elicited at test potentials above −30 mV in cells from both control and MCT-treated rats, and the current amplitude increased almost linearly at more positive potentials. The averaged current-voltage relationships of $I_{to}$ density in 8 control and 13 MCT-treated (hypertrophied) RV cells are shown in Fig. 4*B*. On *day 14*, the $I_{to}$ density (amplitude normalized to $C_m$) of RV cells from MCT-treated rats was significantly larger than that of cells from normal rats. The threshold potential for the activation and the linear current-voltage relationship of $I_{to}$ were, however, unaffected by MCT treatment. Figure 4*C* shows the steady-state activation curves of $I_{to}$. There was no significant difference in the voltage dependence of these curves between control and MCT-treated rats on *day 14*. The steady-state inactivation

Table 2. *Action potential parameters in ventricular cells from control and monocrotaline-treated rats on day 28*

| | $n$ | AMP, mV | RMP, mV | $APD_{25}$, ms | $APD_{50}$, ms | $APD_{90}$, ms |
|---|---|---|---|---|---|---|
| RV cells | | | | | | |
| Control | 14 | 101 ± 4.9 | −75 ± 4.2 | 1.6 ± 0.2 | 6.7 ± 1.2 | 28.3 ± 0.2 |
| MCT | 10 | 103 ± 4.8 | −73 ± 2.9 | 8.4 ± 3.1* | 20.5 ± 5.1* | 49.1 ± 8.4* |
| LV cells | | | | | | |
| Control | 9 | 102 ± 3.0 | −77 ± 5.0 | 3.5 ± 0.7 | 15.0 ± 8.7 | 37.7 ± 3.4 |
| MCT | 10 | 100 ± 5.0 | −75 ± 7.0 | 3.9 ± 2.2 | 16.2 ± 8.3 | 40.8 ± 8.2 |

Values are means ± SE; $n$, no. of cells. MCT, monocrotaline; AMP, amplitude; RMP, resting membrane potential; $APD_{25-90}$, action potential duration at 25, 50, and 90% of repolarization, respectively. *Significantly different from control at $P < 0.05$.

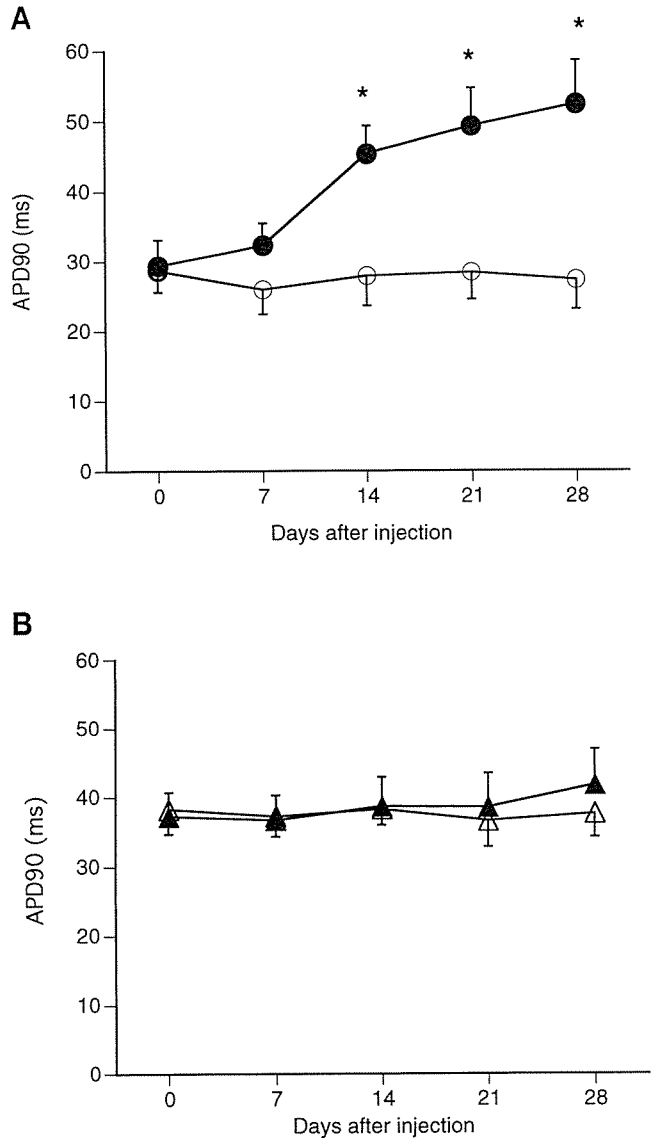


Fig. 3. Sequential changes in action potential duration at 90% of repolarization ($APD_{90}$) of RV (*A*, circles) and LV cells (*B*, triangles) during 4 wk of observation. Values are means ± SE ($n$ = 8–16) obtained from control (open symbols) and MCT-treated (solid symbols) rats. * Significantly different from control at $P < 0.05$.

was also examined with the use of a double-pulse protocol: a conditioning 1-s pulse to various voltage levels (from −100 to 0 mV in 10-mV steps) was followed by a test depolarization to +30 mV. There was no significant difference in the voltage dependence of inactivation between control and MCT-treated rats on *day 14* (Fig. 4C).

Figure 5 shows the results obtained from the rats on *day 28* after injection. Representative recordings of $I_{to}$ were obtained from control and MCT rats with $C_m$ of 90.7 and 101.3 pF, respectively (Fig. 5*A*). At this stage, the $I_{to}$ density of RV cells from MCT-treated rats was significantly lower than that from normal rats (Fig. 5*B*), but the threshold potential for activation and the linear current-voltage relationship were unaffected. The steady-state activation and inactivation curves of $I_{to}$ in control and MCT-treated rats on *day 28* are shown in Fig. 5*C*. There was no significant difference in these curves between the two groups.

Sequential changes of $I_{to}$ density in RV cells from normal and hypertrophied rat hearts are summarized in Fig. 6. In normal rats, the $I_{to}$ density of RV cells was constant throughout the observation period. In MCT-treated rats, the $I_{to}$ density showed biphasic changes: it increased moderately during the initial 2 wk but decreased significantly during the subsequent period. By *day 28*, the average $I_{to}$ density of RV cells from the MCT-treated rats had decreased to 56% of that in the control rats.

*$I_{Ca}$ in normal and hypertrophied myocytes.* Figure 7*A* shows representative recordings of $I_{Ca}$ in RV myocytes from control and MCT-treated rats on *day 14* after injection. $C_m$ was 88.9 pF in the control cell and 93.8 pF in the MCT-treated cell. $I_{Ca}$ was elicited at test potentials above −40 mV, and the current amplitude reached the maximal level at 0 mV depolarization in both control and MCT-treated cells. The average current-voltage relationships of $I_{Ca}$ density in normal and MCT-treated RV cells are summarized in Fig. 7*B*. The $I_{Ca}$ density of RV cells from MCT-treated rats on *day 14* was significantly larger than that of cells from control rats throughout the range of $I_{Ca}$ activation. The average $I_{Ca}$ density at 0 mV in MCT-treated rats (15.7 ± 2.6 pA/pF, $n$ = 10) increased by 55.4% from the value in control rats (10.1 ± 2.3 pA/pF, $n$ = 10). The membrane potentials of the threshold and peak current activation in both groups were essentially the same.

Figure 8*A* shows representative recordings of $I_{Ca}$ in RV myocytes from control and MCT-treated rats on *day 28* after injection. $C_m$ was 86.3 pF in the control cell and 100.2 pF in the MCT-treated cell. The average current-voltage relationships of $I_{Ca}$ density in 10 normal and 10 MCT-treated RV cells are summarized in Fig. 8*B*. There was no significant difference in the $I_{Ca}$ density of RV cells from control (11.6 ± 3.0 pA/pF, $n$ = 10) and MCT-treated rats (8.3 ± 3.7 pA/pF, $n$ = 10) on *day 28*.

The current decay of $I_{Ca}$ was fitted to a double exponential function in each experiment. The time constants of the fast component ($\tau_f$) and the slow component ($\tau_s$) for $I_{Ca}$ inactivation at 0 mV in RV cells from MCT-treated rats on *day 14* after injection ($\tau_f$ = 5.0 ± 0.9 ms, $\tau_s$ = 15.9 ± 3.1 ms, $n$ = 9) were almost identical to those from control rats ($\tau_f$ = 5.1 ± 1.2 ms, $\tau_s$ = 16.8 ± 2.3 ms, $n$ = 12). On *day 28*, the time constants for MCT-treated rats ($\tau_f$ = 5.8 ± 0.9 ms, $\tau_s$ = 20.3 ± 4.6 ms, $n$ = 10) were slightly larger than for controls ($\tau_f$ = 5.3 ± 0.9 ms, $\tau_s$ = 16.9 ± 2.1 ms, $n$ = 10), but the difference did not reach statistical significance.

Figure 9 summarizes the data on $I_{Ca}$ density at 0 mV depolarization on *days 0, 7, 14, 21*, and *28* after injection. In normal rats, the $I_{Ca}$ density of RV cells was constant throughout the observation period. In MCT-treated rats, the $I_{Ca}$ density gradually increased from *day 7* and reached a peak on *day 14*. During the subsequent period, however, the $I_{Ca}$ density decreased and there was no significant

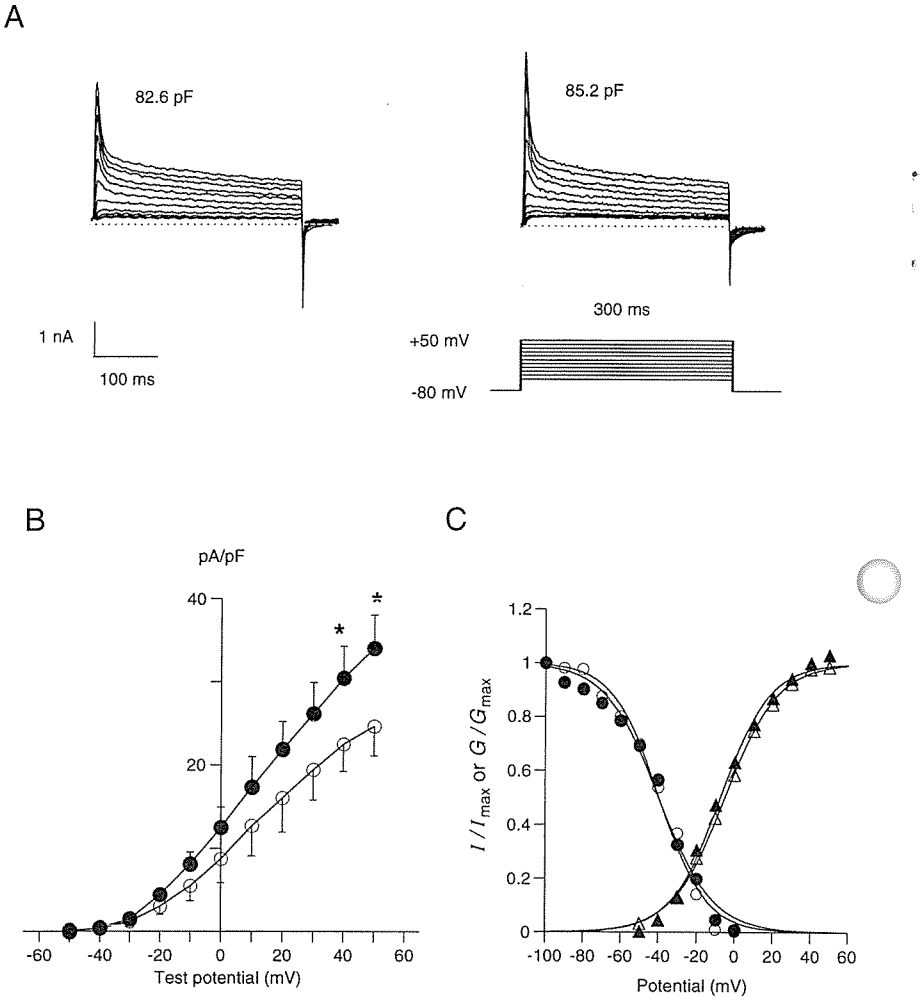


Fig. 4. Transient outward current ($I_{to}$) recorded from RV myocytes on *day 14* after injection. *A*: voltage-clamp protocol and representative current tracings during depolarization steps from a holding potential ($V_h$) of −80 mV to test potentials ranging between −50 and +50 mV (10-mV steps, 300-ms duration) in control (*left*) and MCT-treated hypertrophied (*right*) cells. Cell capacitance ($C_m$) of control and hypertrophied cells were 82.6 and 85.2 pF, respectively. *B*: average peak current density-voltage relationship for $I_{to}$ in control (○, $n$ = 8) and hypertrophied (●, $n$ = 13) myocytes. $I_{to}$ amplitude was divided by $C_m$ in each experiment to obtain $I_{to}$ density (pA/pF). Values are means ± SE. *Significantly different from control at $P < 0.05$. *C*: voltage dependence of steady-state activation and inactivation of $I_{to}$ in control and MCT-treated rat cells. Chord conductance ($G$) was calculated from $I_{to}$ amplitude and plotted against test potential. Mean values obtained from 8 control (△) and 13 MCT-treated rat cells (▲) are shown. Curves are drawn according to Boltzmann equation: $G/G_{max} = 1/[1 + \exp[(V_{0.5} - V)/k]]$, where $V_{0.5}$ is potential at which conductance is half-maximally activated and $k$ is a slope factor describing steepness of activation curve. $V_{0.5}$ and $k$ were −4.3 mV and 13.9 in control and −5.7 mV and 13.6 in MCT-treated cells. Steady-state inactivation was examined with a double-pulse protocol: a conditioning 1-s pulse to various voltage levels (from −100 to 0 mV in 10-mV steps) was followed by a test depolarizing pulse to +30 mV. Normalized $I_{to}$ amplitude was plotted against conditioning potential. Mean values obtained from 10 control (○) and 9 MCT-treated rat cells (●) are shown. Curves are drawn according to Boltzmann equation: $I/I_{max} = 1/[1 + \exp[(V - V_{0.5})/k]]$, where $V_{0.5}$ and $k$ are −39.6 mV and 12.3 in control and −39.8 mV and 14.1 in MCT-treated cells.

difference from the control on *days 21* and *28*. The current-voltage relationships of $I_{Ca}$ density on *days 21* and *28* were also unchanged by the MCT treatment.

*Direct effects of MCT on ventricular myocytes.* Direct effects of MCT on action potential configuration were examined in vitro in each of four RV and LV cells isolated from control rats. Bath application of MCT at concentrations ranging from 1 to 60 mg/l caused no significant changes in RMP, AMP, $APD_{25}$, $APD_{50}$, or $APD_{90}$ of the myocytes stimulated at 1.0 Hz. Direct effects of MCT on $I_{to}$ and $I_{Ca}$ were tested in each of five RV cells from control rats. Bath application of MCT (1–60 mg/L) resulted in no significant changes in amplitude and current-voltage relationship of these ionic currents (data not shown).

## DISCUSSION

In the present study, we investigated time courses of changes in action potential configuration and the density of $I_{to}$ and $I_{Ca}$ in ventricular myocytes isolated from rat hearts with RV hypertrophy secondary to MCT-induced pulmonary hypertension. After MCT treatment, all the rats injected with this compound showed a macroscopic hypertrophy of RV from the second week without any morphological changes in the LV. At the end of the fourth week, most of the MCT-treated rats showed obvious signs of right-side heart failure and inhibition of normal growth, and most of them died in the fifth to sixth weeks. In association with the development of hypertrophy, cell membrane capacitance and APD of RV cells increased progressively, whereas other parameters of the action potential (resting membrane potential and action potential amplitude) were unaffected. The $APD_{90}$ of the MCT-treated RV cells was prolonged to 162.7 and 192.1% of control on *days 14* and *28*, respectively. These changes in cell membrane capacitance and action potential configuration are qualitatively similar to previous reports on other models of rat ventricular hypertrophy.

MCT causes pulmonary hypertension in rats through endothelial cell damage, medial thickening of the muscular pulmonary arteries, and neomuscularization of nonmuscular distal arteries. Recent experimental studies have indicated that an increase of endogenous endothelin-1 (ET-1), a potent endothelium-derived vasoconstrictor peptide, is involved in the pathogenesis of MCT-induced pulmonary hypertension (19, 22). Endogenous ET-1 is also present in the heart, and the peptide was shown to induce myocardial cell hypertrophy and to have positive inotropic and chronotropic effects (11,

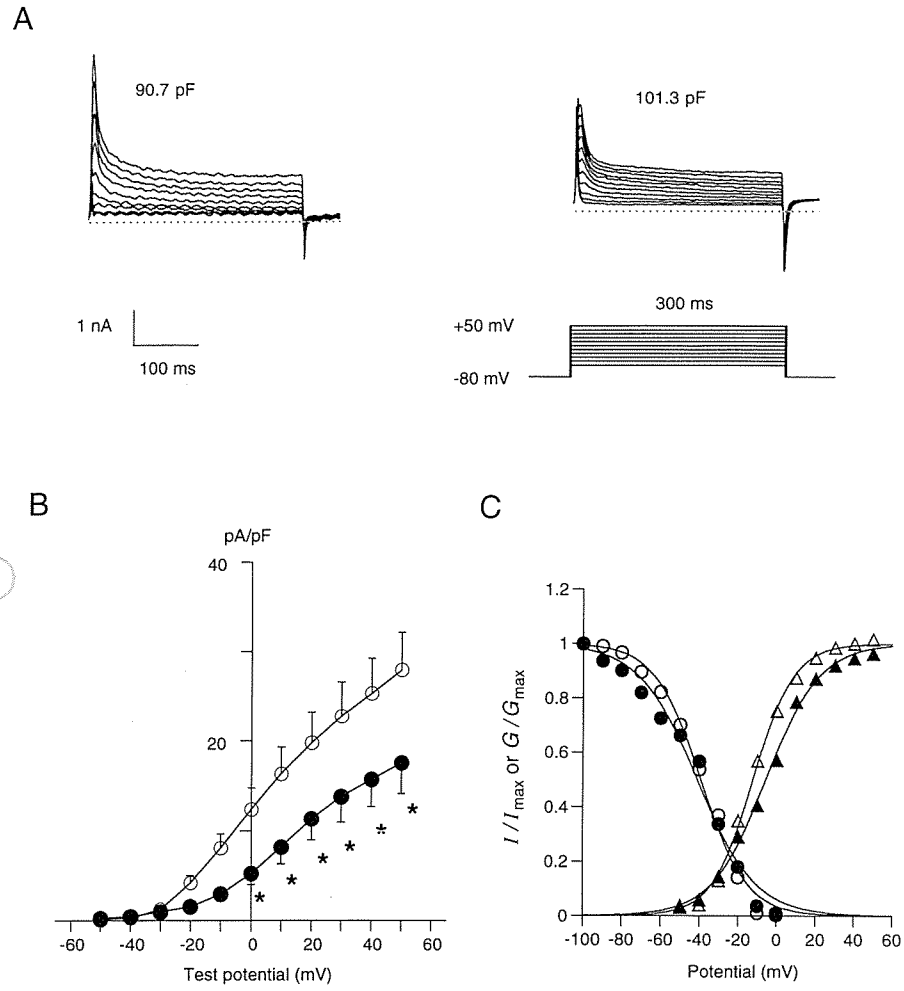


Fig. 5. $I_{to}$ recorded from RV myocytes on *day 28* after injection. *A*: voltage-clamp protocol and representative current tracings with same protocol used on *day 14*. $C_m$ of control (*left*) and hypertrophied (*right*) cells were 90.7 and 101.3 pF, respectively. *B*: average peak current density-voltage relation for $I_{to}$ in control (○, $n$ = 10) and hypertrophied (●, $n$ = 9) myocytes with same protocol used on *day 14*. Values are means ± SE. *Significantly different from control at $P < 0.05$. *C*: steady-state activation (triangles) and inactivation (circles) of $I_{to}$ in control (open symbols) and MCT-treated (solid symbols) rat cells. Mean values from 7–10 rats were shown. $V_{0.5}$ and $k$ for steady-state activation were −12.3 mV and 10.5 in control and 14.2 mV and −5.2 in MCT-treated rats. $V_{0.5}$ and $k$ for steady-state inactivation were −39.3 mV and 12.0 in control and −40.8 mV and 14.9 in MCT-treated rats.

23). Accordingly, the MCT-induced ventricular hypertrophy could be mediated in part by a direct action of ET-1 on ventricular myocytes. In the present model of hypertrophy, however, this possibility is unlikely, because $C_m$ and the APD of LV cells were unaffected by MCT treatment throughout the entire period of observation. Bath application of MCT had no direct effects on the action potential configuration and on the ionic currents ($I_{to}$ or $I_{Ca}$). All the electrophysiological changes in the hypertrophied ventricular myocytes presented in this paper, therefore, may have been induced primarily by RV pressure overload.

The present results have revealed complex, stage-dependent changes in $I_{to}$ and $I_{Ca}$ in hypertrophied ventricular cells, which may explain the discrepancies among previous reports. In rat myocytes in which hypertrophy was secondary to increased growth hormone secretion (29), sustained pressure overload produced by aortic constriction (3, 28), deoxycorticosterone acetate salt-induced hypertension, or genetically determined hypertension (6), $I_{to}$ density was shown to decrease compared with respective controls. However, a significant increase in $I_{to}$ density was reported by Ten Eick et al. (27) for hypertrophied RV myocytes from cats with pulmonary artery banding and by Li and

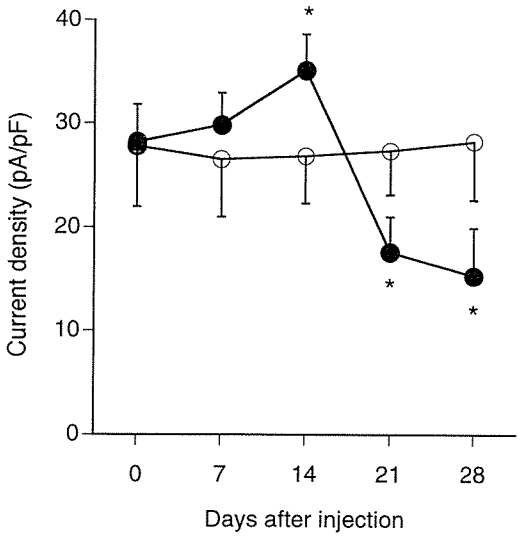


Fig. 6. Sequential changes in $I_{to}$ density of RV cells during 4-wk observation period. Values are means ± SE ($n$ = 8–16) obtained from control (○) and MCT-treated rats (●). *Significantly different from control at $P < 0.05$.

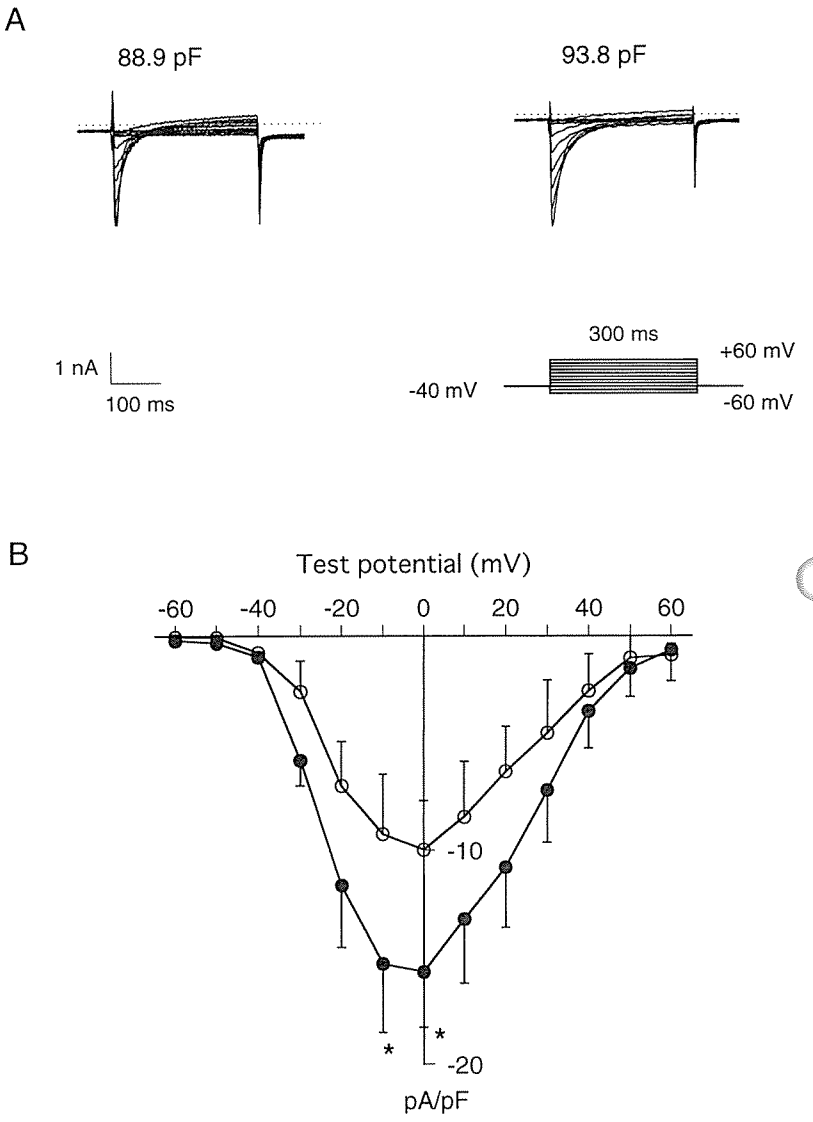


Fig. 7. L-type calcium current ($I_{Ca}$) recorded from RV myocytes on *day 14* after injection. *A*: voltage-clamp protocol and representative current tracings during depolarization steps from a $V_h$ of −80 mV to test potentials ranging between −60 and +60 mV (10-mV steps, 300-ms duration) in control (*left*) and MCT-treated hypertrophied (*right*) cells. $C_m$ of control and hypertrophied cells were 88.9 and 93.8 pF, respectively. *B*: average peak current density-voltage relationship for $I_{Ca}$ in control (○, $n$ = 10) and hypertrophied (●, $n$ = 10) cells. $I_{Ca}$ amplitude was divided by $C_m$ in each experiment to obtain $I_{Ca}$ density (pA/pF). Values are means ± SE. *Significantly different from control at $P < 0.05$.

Keung (15) for LV hypertrophied myocytes from rats with renovascular hypertension. It was shown in cats with RV or LV hypertrophy produced by aortic constriction that peak $I_{Ca}$ of hypertrophied myocytes was not different from control groups, but its inactivation kinetics were delayed (7, 14). Similar findings have been reported in myocytes from rats with aortic stenosis (26). In Goldblatt hypertrophied rat myocytes (13) and in slightly hypertrophied guinea pig myoctes (25), however, the peak $I_{Ca}$ was shown to increase. In RV myocytes from cats with severe RV hypertrophy (21) and in LV myocytes from hypertrophied failing guinea pig hearts (17), $I_{Ca}$ density was shown to be reduced. Such different responses cannot be attributed solely to species differences or to different stimuli to induce hypertrophy, because different results have been found in hypertrophied RV myocytes from cats with pulmonary artery banding (14, 21) and in LV myocytes from guinea pigs with aortic constriction (17, 25).

In a recent comprehensive review of cellular electrophysiology in cardiac hypertrophy and failure, Hart (9) analyzed 16 different studies on $I_{Ca}$ density of hypertrophied ventricular cells in terms of the possible relationship between the direction of the change and severity of hypertrophy. He graded the hypertrophy into three groups: mild, moderate, and severe. Hypertrophy of either ventricle with an increase in heart-to-body weight ratio <15% was defined as mild, and a ratio >20% was defined as moderate. Cases with the presence of congestion proximal to the affected chambers associated with any degree of cardiac hypertrophy were defined as severe. On the basis of this definition, two studies in which mean $I_{Ca}$ density was 30% higher than control involved mild hypertrophy of the RV or the LV (12, 15). Three studies in which mean $I_{Ca}$ density was reduced were characterized by severe chamber hypertrophy and heart failure (17, 21, 24), and most of the remaining studies showing no significant changes in $I_{Ca}$ density were characterized by moderate hypertrophy. Therefore, the following conclusion was proposed. In mild hypertrophy, $I_{Ca}$ density may be increased; in moderate

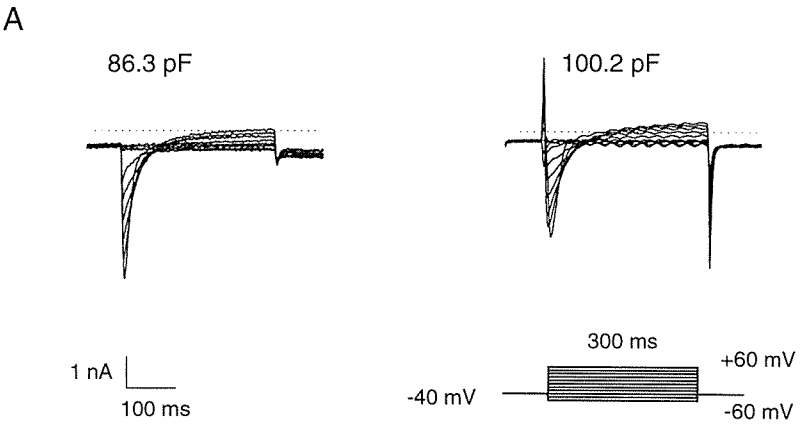


Fig. 8. $I_{Ca}$ recorded from RV myocytes on *day 28* after injection. *A*: voltage-clamp protocol and representative current tracings with same protocol used on *day 14*. $C_m$ of control (*left*) and hypertrophied (*right*) cells were 86.3 and 100.2 pF, respectively. *B*: average peak current density-voltage relationships for $I_{Ca}$ of control (○, $n$ = 10) and hypertrophied (●, $n$ = 10) cells. Values are means ± SE.

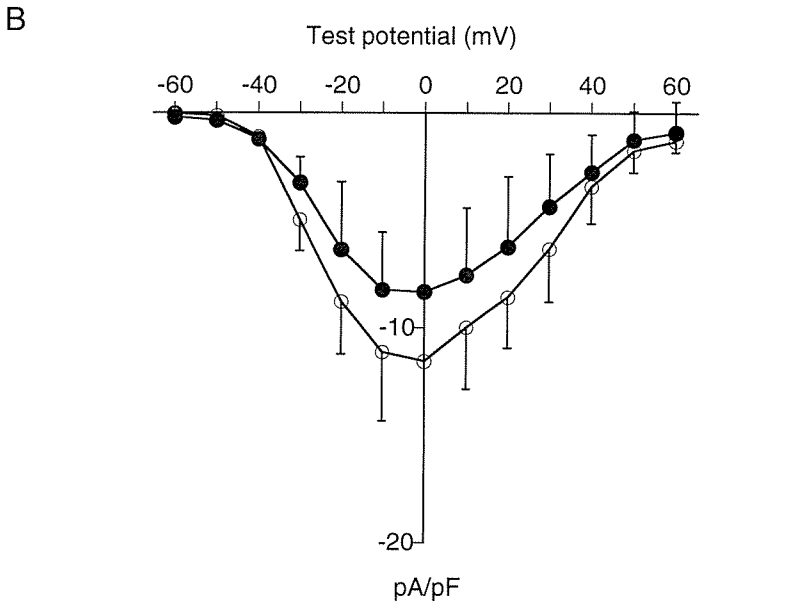


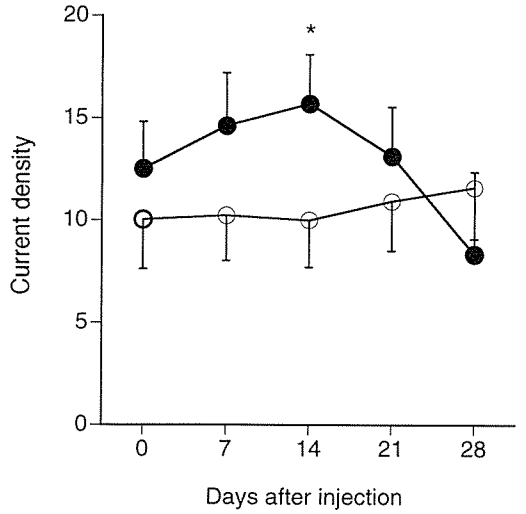


Fig. 9. Sequential changes in $I_{Ca}$ density of RV cells during 4-wk observation period. Values are means ± SE ($n$ = 8–10) obtained from control (○) and MCT-treated rats (●). *Significantly different from control at $P < 0.05$.

degrees of hypertrophy, $I_{Ca}$ density is usually unchanged; and in severe hypertrophy with failure, $I_{Ca}$ density is usually reduced.

The present results on ionic currents are essentially concordant with the proposal by Hart (9) in terms of the stage dependence. The APD prolongation in the early compensated stage of hypertrophy may be caused mainly by an increase in $I_{Ca}$ density. In the late decompensated stage of hypertrophy, however, a decrease in $I_{to}$ density may account for the further APD prolongation. A computer simulation of action potentials with a model of ionic currents would be helpful to substantiate this idea.

The stage-dependent changes in the macroscopic $I_{to}$ and $I_{Ca}$ observed in the present study may be the result of a change in structure and function of normally expressed channels, a change in the number of functional channels, or a combination of both. Further experimental studies of the single channel properties and the gene expression of channel proteins are required to clarify this issue.

The authors thank Dr. James N. Weiss for helpful comments on the manuscript and Dr. Atsushi Ozawa for useful advice on the animal model.

Address for reprint requests: I. Kodama, Dept. of Humoral Regulation, Research Institute of Environmental Medicine, Nagoya Univ., Furo-cho, Chikusa-ku, Nagoya 464–01, Japan.

Received 31 July 1996; accepted in final form 3 February 1997.

## REFERENCES


1. **Apkon, M., and J. M. Nerbonne.** Characterization of two distinct depolarization-activated $K^+$ currents in isolated adult rat ventricular myocytes. *J. Gen. Physiol.* 97: 973–1011, 1991.
2. **Aronson, R. S.** Characteristics of action potentials of hypertrophied myocardium from rats with renal hypertension. *Circ. Res.* 47: 443–454, 1980.
3. **Bénitah, J.-P., A. M. Gomezu, P. Bailly, J.-P. Da Ponte, G. Berson, C. Delgado, and P. Lorente.** Heterogeneity of the early outward current in ventricular cells isolated from normal and hypertrophied rat heart. *J. Physiol. (Lond.)* 469: 111–138, 1993.
4. **Beuckelmann, D. J., M. Nabauer, and E. Erdmann.** Alteration of $K^+$ currents in isolated human ventricular myocytes from patients with terminal heart failure. *Circ. Res.* 73: 379–385, 1993.
5. **Brooksby, P., A. J. Levi, and J. V. Jones.** The electrophysiological characteristics of hypertrophied ventricular myocytes from the spontaneous hypertrophied rat. *J. Hypertens.* 11: 611–622, 1993.
6. **Cerbai, E., M. Barbieri, Q. Li, and A. Mugelli.** Ionic basis of action potential prolongation of hypertrophied myocytes isolated from hearts of spontaneously hypertensive rats of different ages. *Cardiovasc. Res.* 28: 1180–1187, 1994.
7. **Furukawa, T., R. J. Myerburg, N. Furukawa, S. Kimura, and A. L. Bassett.** Metabolic inhibition of $I_{Ca,L}$ and $I_K$ differs in feline left ventricular hypertrophy. *Am. J. Physiol.* 266 (*Heart Circ. Physiol.* 35): H1121–H1131, 1994.
8. **Hamill, O. P., A. Marty, E. Neher, B. Sakmann, and F. J. Sigworth.** Improved patch-clamp techniques for high-resolution current recording from cells and cell-free membrane patches. *Pflügers Arch.* 391: 85–100, 1981.
9. **Hart, G.** Cellular electrophysiology in cardiac hypertrophy and failure. *Cardiovasc. Res.* 28: 933–946, 1994.
10. **Hayashi, Y., J. F. Hussa, and J. J. Lalich.** Cor pulmonale in rats. *Lab. Invest.* 16: 875–881, 1967.
11. **James, A. F., L. H. Xie, Y. Fujitani, S. Hayashi, and M. Horie.** Inhibition of the cardiac protein kinase A-dependent chloride conductance by endothelin-1. *Nature* 370: 297–300, 1994.
12. **Keung, E. C., and R. S. Aronson.** Nonuniform electrophysiologic properties and electrotonic interaction in hypertrophied rat myocardium. *Circ. Res.* 49: 150–158, 1981.
13. **Keung, E. C.** Calcium current is increased in isolated adult myocytes from hypertrophied rat myocardium. *Circ. Res.* 64: 753–763, 1989.
14. **Kleiman, R. B., and S. R. Houser.** Calcium currents in normal and hypertrophied isolated feline ventricular myocytes. *Am. J. Physiol.* 255 (*Heart Circ. Physiol.* 24): H1434–H1442, 1988.
15. **Li, Q., and E. C. Keung.** Effects of myocardial hypertrophy on transient outward current. *Am. J. Physiol.* 266 (*Heart Circ. Physiol.* 35): H1738–H1745, 1994.
16. **Lukas, A., and C. Antzelevitch.** Differences in the electrophysiological response of canine ventricular epicardium and endocardium to ischemia. Role of the transient outward current. *Circulation* 88: 2903–2915, 1993.
17. **Ming, Z., C. Noedin, F. Siri, and R. S. Aronson.** Reduced calcium current density in single myocytes isolated from hypertrophied failing guinea pig heart. *J. Mol. Cell. Cardiol.* 26: 1133–1143, 1994.
18. **Mattocks, A. R.** Toxicity of pyrrolizidine alkaloids. *Nature* 217: 723–728, 1968.
19. **Miyauchi, T., R. Yorikane, S. Sakai, T. Sakurai, M. Okada, M. Nishikibe, M. Yano, I. Yamaguchi, Y. Sugita, and K. Goto.** Contribution of endogenous endothelin-1 to the progression of cardiopulmonary alterations in rats with monocrotaline-induced pulmonary hypertension. *Circ. Res.* 73: 887–897, 1993.
20. **Nabauer, M., D. J. Beuckelmann, and E. Erdmann.** Characteristics of transient outward current in human ventricular myocytes from patients with terminal heart failure. *Circ. Res.* 73: 386–394, 1993.
21. **Nuss, H. B., and S. R. Houser.** Voltage dependence of contraction and calcium current in severely hypertrophied feline ventricular myocytes. *J. Mol. Cell. Cardiol.* 23: 717–726, 1991.
22. **Okada, M., C. Yamashita, M. Okada, and K. Okada.** Role of endothelin-1 in beagles with dehydromonocrotaline-induced pulmonary hypertension. *Circ. Res.* 92: 114–119, 1995.
23. **Ono, K., G. Tsujimoto, A. Sakamoto, K. Eto, T. Masaki, Y. Ozaki, and M. Satake.** Endothelin-A receptor mediates cardiac inhibition by regulating calcium and potassium currents. *Nature* 370: 301–304, 1994.
24. **Rossner, K. L.** Calcium current in congestive heart failure of hamster cardiomyopathy. *Am. J. Physiol.* 260 (*Heart Circ. Physiol.* 29): H1179–H1186, 1991.
25. **Ryder, K. O., S. M. Bryant, and G. Hart.** Membrane current changes in left ventricular myocytes isolated from guinea pigs after abdominal aortic coarctation. *Cardiovasc. Res.* 27: 1278–1287, 1993.
26. **Scamps, F., E. Mayoux, D. Charlemagne, and G. Vassort.** Calcium current in single cells isolated from normal and hypertrophied rat heart. Effects of β-adrenergic stimulation. *Circ. Res.* 67: 199–208, 1990.
27. **Ten Eick, R. E., K. Zhang, R. D. Harvey, and A. L. Bassett.** Enhanced functional expression of transient outward current in hypertrophied feline myocytes. *Cardiovasc. Drugs Ther.* 7: 611–619, 1993.
28. **Tomita, F., A. L. Bassett, R. J. Myerburg, and S. Kimura.** Diminished transient outward currents in rat hypertrophied ventricular myocytes. *Circulation* 75: 296–303, 1994.
29. **Xu, X., and P. M. Best.** Decreased transient outward $K^+$ current in ventricular myocytes from acromegalic rats. *Am. J. Physiol.* 260 (*Heart Circ. Physiol.* 29): H935–H942, 1991.